Renewable Energy 131 (2019) 763–777

Contents lists available at ScienceDirect

Renewable Energy

journal homepage: www.elsevier.com/locate/renene

Efficient workflow for simulation of multifractured enhanced geothermal systems (EGS)

Pranay Asai*, Palash Panja, John McLennan, Joseph Moore

University of Utah, Salt Lake City, USA

ARTICLE INFO

Article history:
Received 15 February 2018
Received in revised form
12 July 2018
Accepted 15 July 2018
Available online 19 July 2018

Keywords:
Simulation issues
Enhanced geothermal system (EGS)
Up-scaling
Doublet Well System
Grid sensitivity
Fracture transmissivity

ABSTRACT

The increasing demand for clean energy with minimum environmental impact motivates development of geothermal energy. Simulating a geothermal reservoir is complex and time consuming, mainly because of the systems spatial and temporal non-isothermal nature and the enormous size of the domain/reservoir. Simulations become even more complex when representing Enhanced Geothermal Systems (EGS), where wells in a hot, low permeability reservoir are interconnected by hydraulic fracturing to provide pathways for injection of cold water, in situ heating, and consequent production of hot water. In this study, various issues related to simulation of enhanced geothermal systems are investigated and practical solutions are proposed. A comprehensive study was conducted to show the effect of different grid systems on predictions of the transient temperature of the produced water. It is shown that the performance of an EGS is affected by the transmissivity (product of permeability and width of the fracture) of the fracture more so than by the values of permeability and width of the fracture considered individually. A simplified model (downscaled model) reduces the simulation times significantly (by 1.5 −14.5 times) without compromising the accuracy of the results. In the proposed model, only two simulations - capturing small portions of the top and bottom of a reservoir with two active hydraulic fractures is used to evaluate performance of the entire reservoir. The proposed model is proved to be robust when exposed to different scenarios created by varying the inclination of the wells with respect to horizontal, spacing of the hydraulic factures, and spacing between the injection and producing wells. Value of R^2 close to unity (0.96−1.0) and smaller value of MAPE (Mean Absolute Percentage Error), less than 3% in comparison to the entire reservoir simulations, indicate the utility of proposed model.

© 2018 Elsevier Ltd. All rights reserved.

1. Introduction

Geothermal energy extraction from hot dry rock (HDR) has been considered feasible for more than fifty years. Duchane et al. [1] mentions that the technology to access the HRD resource and to bring the heat to the surface was developed by group of scientist at Los Alamos National Laboratory, as early as in 1970. In 1978, Smiths et al. [2] performed seismic study on single and dual well systems to detect fractures in the artificial geothermal reservoir to study the heat extraction. A. S. Batchelor [3] evaluated the potential of HRD in the UK in 1982 and stressed that it can be used as a potential source of energy. In 1989, Tester et al. [4] created a report to describe the nature of HDR resources and conceptualize the technology to use the produced heat in several applications. After all these years of research and developments in the geothermal realm, it still has many unresolved issues and unanswered questions.

Rebranded today as Enhanced Geothermal Systems (EGS) [5] there is revived interest in this field and a new perspective on recovering heat from an adequately hot thermal reservoir at shallow depth by creating an artificial circulation system. EGS entails using hydraulic fracturing and stimulation to create highly conductive zones that interconnect an injection well to a production well, forming a doublet system. The commercial potential of a geothermal reservoir as an EGS candidate is determined by the temperature, depth, geothermal gradient, and the extent of the reservoir. The thermal attributes such as heat capacity and thermal conductivity along with the geologic properties also influence the ability to effectively create a hydraulic system.

Planning and exploiting an EGS is a huge capital investment. Drilling and reservoir development costs are substantial as are

* Corresponding author. Energy & Geoscience Institute, The University of Utah, 423 Wakara Way, Suite #300, Salt Lake City, UT 84108, USA.
E-mail addresses: pasai@egi.utah.edu (P. Asai), ppanja@egi.utah.edu (P. Panja), jmclennan@egi.utah.edu (J. McLennan), jmoore@egi.utah.edu (J. Moore).

https://doi.org/10.1016/j.renene.2018.07.074
0960-1481/© 2018 Elsevier Ltd. All rights reserved.

installing surface facilities for electric generation, transmission lines, and other infrastructure. To justify such expenditures, a reliable method for forecasting long term production and thermal energy is essential [6]. Thus, simulation of heat recovery from EGS plays becomes essential for predicting heat extraction, thermal depletion and longevity of the resource. Multiple simulations, recognizing variations in in-situ reservoir data are required to identify efficient protocols to optimize the heat extraction from the reservoir and minimize economic risk. A geothermal system with a good thermal gradient (greater than 60–65 °C/km) at a relatively shallow depth (2–4 km) with an in-situ temperature of 200 °C, is considered to be an economically viable target in terms of energy recovery.

Extensive evaluations have assessed heat extraction for different conceptual subsurface designs. The most elementary system would be a doublet (with one production and one injection well) or a triplet (two production and an injection wells). These wells, ideally drilled at a high angle to the vertical, would need to be interconnected by artificially generated fractures in the reservoir or by reactivating fractures that already existed. Usually multiple fractures are created to enhance the flow in the reservoir. The favored method for creating/reactivating fractures is by hydraulic injection. When the injection/production wells are drilled horizontally and fractured, all of the fractures should ideally lie in the same temperature zone. For such system, simulating a small section and scaling it up to the entire reservoir is not an issue as all the fractures (if equally spaced) can be considered identical and the system can be scaled up linearly. But when the wells are vertical or inclined, scaling up using a single fracture, would not yield correct results because the temperature keeps changing with depth and each fracture would lie in a different temperature zone. Xia et al. [7] studied the effect of fracture spacing for doublet horizontal and inclined wells interconnected by group of five hydraulic fractures along the well and then scaling it up for the entire reservoir, without mentioning how they scaled it up for the angular wells. Aliyu et al. [8] considered the effects of injection flow rate, fluid injection temperature, and lateral well spacing on just one fracture. Zeng et al. [9] studied heat extractions with two-dimensional fracture modeling and concluded that the EGS is sensitive to flow rate and injection temperature, as would be expected. The simulation protocols were not disclosed. Huang et al. [10] studied EGS performance and concluded that heterogeneity plays an important role in recovery and longevity and the temperature decline is affected by the fluid losses in the reservoir. They argued that permeability of the reservoir itself in addition to the transmissivity of the hydraulic fractures was relevant. As for the modeling and simulation part Zhang et al. [11] proposed a new conceptual model for the field of Chingshui geothermal field in Taiwan, by changing the existing model and running it using TOUGH. But due to the larger size of the model (3250 m × 4800 m), they had to use larger grid sizes (10 m × 50 m) to avoid the computational overhead. Whereas, Wu et al. [12] developed a semi-analytical model using Laplace transform and conjugate function to predict the temperature decline curve for a closed loop geothermal system. Though they were able to address the major issues related to simulation of a multifracted EGS by developing complex flow equations, they didn't talk much about different geometry of the wells in the reservoir. Song et al. [13] also developed analytical equations to predict the performance of the EGS in a closed loop system, but even they didn't address the concerns related to proper gridding of the reservoir and the computational load required to run those simulations. Although all these and other studies with hypothetical model developments have helped in developing a better understanding of the heat extraction, none of them specifically address the challenges in modeling and simulation of an EGS.

This study focuses on the solving the issues related to simulation and developing simplified model. We have considered the hurdles encountered in modeling the heat extraction from a geothermal reservoir and suggested protocols to resolve them. The rudimentary system adopted considers two parallel wells, connected by multiple planar rectangular hydraulic fractures (doublet system). A working fluid (usually water) is circulated through the system to extract heat to the surface. We simulated this EGS using commercial reservoir modeling software, CMG STARS [14].

2. Simulation of enhanced geothermal system

There are many well configurations (doublet, triplet etc.) can be conceived for studying the heat recovery from an EGS. In this study, a doublet system is considered. A schematic diagram of a doublet with one transverse[1] vertical fracture connecting the production well and injection well is shown in Fig. 1.

Ideally, in EGS we try to maximize the exposure to high temperature reservoir and afford a good opportunity for interconnection by hydraulic fracturing. EGS experience indicates that subhorizontal to horizontal wells will be appropriate for this. By convention, a well's inclination is measured from the vertical axis, as shown in Fig. 1(a). Well spacing is measured as the perpendicular distance between the two wells, whereas fracture spacing is the horizontal spacing between two consecutive fractures. Typically, the injection well is conceived to be placed below the production well so that the injected water flows upward from the higher temperature region towards the lower temperature production well. Injected water is distributed among multiple vertical fractures according to different pressures in the fractures along the length of the horizontal well. Heat transfer between the fluid and the reservoir takes place inside the fracture, dominantly by convection and conduction (Fig. 1(b)). Heat flows within the reservoir (towards the fracture) as the working fluid extracts the heat from the fracture.

The main aim of this study was to establish if the modelling of the entire reservoir could be downscaled (using just couple of fractures instead of all) and after running the simulation, upscaling back the results (without actually having to simulate the entire domain) to predict the temperature decline curve for the entire reservoir. A protocol for this downscaling was evaluated and the downscaled model (here after referred as proposed model) was tested over wide range of input to check if it was flexible enough to incorporate changes in well spacing, fracture spacing and the angle of well. This model will save time in design and execution of the simulations and modeling and remove the requirements for excessive computational capacity. Conversely, the physics of simultaneous heat and mass transfer in geothermal system and impacts of various parameters (well spacing, fracture spacing, injection rate etc.) on amount of heat extracted are discussed in a previous article [15]. The flow of this research has been highlighted in the Fig. 2.

The experiment composes of three major steps; input, processing and output. Before we start designing the simulation model we need to get data about the reservoir (permeability, porosity, heat conductivity etc.), completion data (number of wells, angle of inclination, fracture spacing, etc.) and the operational data (injection flow rate, type of injection fluid, injection temperature, etc.). Three sections, marked by red dotted lines in the Fig. 2, are described later to elaborate the issues of grid size in simulation and

[1] In hydraulic fracturing terminology, a transverse fracture is assumed to be orthogonal to the well from which it was created (an axial fracture would propagate along the length of the well).

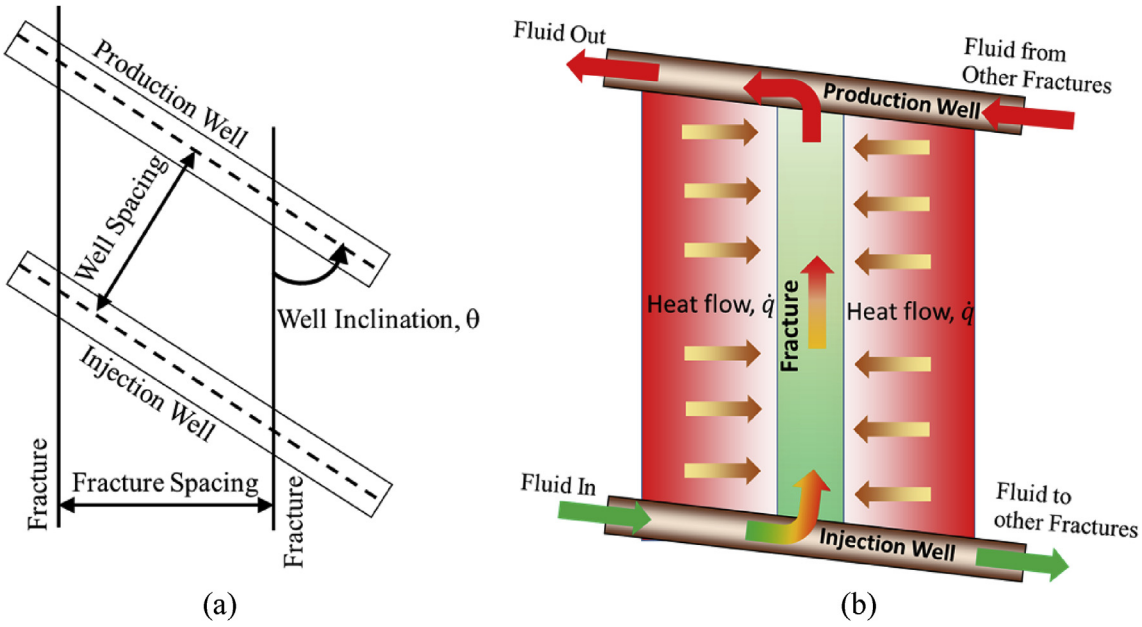

Fig. 1. (a) Schematic diagram of well and fracture trajectories for a doublet EGS, (b) Schematic diagram of an EGS showing fluid and heat flow in the fracture.

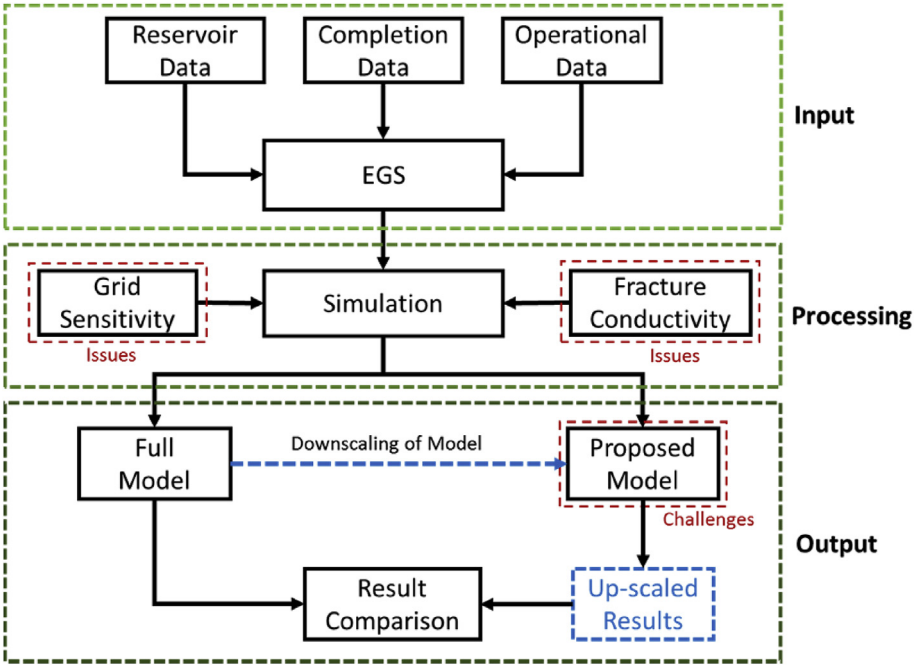

Fig. 2. The study and the structure of this article.

the conductivity of hydraulic fracture and the challenges to develop a simulation scheme to downscale the entire reservoir. The need for proper gridding [16] of the reservoir is also discussed in this study to get accurate results by dividing the reservoir into small blocks. A compromise is always desirable to avoid excessive gridding and computational overhead. Also how transmissivity of the fractures affect the flow through them and the heat extraction, is also studied. The transmissivity of a fracture is defined as the product of the average width of the facture times the permeability of the fracture.

As shown in Fig. 2, to get the simulation ready we need to obtain the parameters to build up the simulation model, which include getting reservoir, completion and operational data. The reservoir parameters used in this study were approximately based on reservoir data from the U.S. Department of Energy's Frontier Observatory for Research in Geothermal Energy (FORGE) site near Milford, Utah. The nominal temperature gradient at this site is 60 °C/km of vertical depth with a reference temperature of 200 °C at a true vertical depth of 2500 meters. The granodiorite reservoir is low porosity (1% or less) and low permeability (on the order of 30 micro Darcies). The lateral length of the wells is approximately a kilometer with possibly ten to fifty hydraulic fractures

interconnecting the two wells (injection well and production well). One proposed well configuration is a doublet, with each well 1000 m long at an inclination of 60°. From a practical point of view, these wells are initially drilled vertically down to a kickoff depth of approximately 1460 m. At this depth the drill bit is forced to drill on a controlled radius of curvature until the bit is at an angle of 60° to the vertical. Continued drilling will follow this 60° trajectory for 1000 m. For a 100 m fracture spacing, approximately 11 hydraulic fractures are required and each fracture connects the injection and production wells for circulation of the injected water. The completion and operational data was acquired from the previous study on heat optimization [15].

A commercial simulator, STARS from Computer Modeling Group (CMG) based in Calgary Canada, is used for reservoir simulation to study heat and mass transfer. STARS is a three-phase, three-dimensional, multi-component thermal simulator. It is widely used to simulate geothermal reservoir to study the heat and fluid flow inside the reservoir [15,17–19]. It uses fully implicit and adaptive implicit methods for numerical solution of reservoir models with Cartesian, cylindrical, or variable depth/variable thickness grid systems. Heat transfer between the reservoir and the working fluid is dominantly a function of the temperature difference, flow rate and the surface area of the fractures.

The size of grid is one of the sensitive parameters which affects the accuracy of the results from the numerical solution. The time discretization is not explicitly defined for entire time period in the simulations. However, the minimum (10^{-8} day) and maximum (20 day) time steps are provided by users. Detailed discussion of the numerical solution method for the heat and fluid transfer is given in STARS user manual [14]. One point where CMG STARS falls short is that it does not have a sophisticated way to simulate finite aperture, high conductivity fracture with irregular dimensions. According to Gringarten et al. [20], the interconnecting fractures can be considered to be rectangular and planar with a surface area approximating an actual hydraulic fracture. This simplification facilitates evaluating heat extraction from one or more fracture in the EGS. As it is standard in many reservoir simulations, these fractures were mimicked by using small but high permeability cells and with higher porosity than the surrounding reservoir. These amalgamated cells emulate fractures. All of the simulated factures were assumed to be uniform and isotropic with the same fracture transmissivity. Naturally, this is an approximation. Fracture transmissivity is also not static; it will increase as the fracture aperture increases with decreasing near-fracture temperature along the fracture length. The heat transfer inside the fracture is dominantly a function of the total surface area of the fracture participating in the flow from one point source to another (Shook et al. [21]). As long as the surface area is same, these simplifications allow us to consider a rectangular planar fracture instead of the complex fracture network.

Once all the data is acquired we move towards designing the simulation model. While designing the model, we usually encounter some challenges and issues especially when it comes to deciding the gridding of the system or to decide on the width/transmissivity for the fractures. In this study, these two major issues were researched individually to come up with an efficient solution so as to optimize the model.

2.1. Grid sensitivity

Grid sensitivity is often modeler's first consideration. The model created in the CMG enfranchises small cells, and each individual cell is isotropic. The properties and the initial conditions are defined individually for the cells at the start of the simulation. Fewer, larger cells may not be able to represent the reservoir accurately, especially when there is a significant temperature gradient in the reservoir. Reducing the cell sizes, and the consequent increase in the number of cells, can provide a better representation of the actual reservoir. However, this comes at the cost of increased time for initialization, running, and processing. An optimization study was undertaken to assess the effect of cell size.

Different grids in all the directions can be defined individually according to the Cartesian coordinate system. This allows us to get refinement in the desired direction. The grids along the z-axis need to be refined in the EGS model in order to represent temperature in the reservoir more accurately due to geothermal gradient. The grids along the y-axis need refinement as well because of the fluid movement in the y-z plane, where the convective and conductive heat transfers take place between the reservoir and the fluid. Whereas the fluid flow along the x-axis is almost negligible and the heat transfer within the reservoir is dominantly due to conduction, which depends only on the temperature gradient. Hence the grids along the x-axis can be bit coarser than those along y-axis or z-axis. For example, a diagram showing the progressive refinement of grids from coarse to fine along x-z plane is shown in Fig. 3.

The number of cells can also be optimized by using a smart technique by having variable cell sizes across the reservoir as previously demonstrated by Sanyal et al. [22]. To implement this, first we need to identify the highly-dynamic zones inside the reservoir. Smaller cells are needed to represent the highly-dynamic locations such as near the fracture zone and the wellbores, because of the huge gradient in the properties of the grids (mainly porosity, permeability, and temperature). These zones are highly susceptible to small changes, hence smaller cells would help resolve the changes in a better way. But as we move away from these dynamic zones, the changes are diluted down and hence coarser cells can be used. Therefore, instead of having uniform grids, it is beneficial to have the varying grid spacing, which are finer near the highly-dynamic zones but become coarser away from them (Fig. 4). This helps in reducing the total number of cells and hence reducing the computational time.

To understand the effect of cell size in a better way five different grids for each x, y, and z direction were studied. Thirteen simulations were carried out with a base case (simulation number S3) consisting of 58, 77 and 367 cells in x, y and z direction respectively as shown in Table 1 (marked as bold). The base case was chosen in such a way that it gave proper results with minimum or acceptable errors and would also require less run time.

Simulations S1 through S5 were intended to study the effect of refinement in x-direction, where the number of cells in the x direction is varied, keeping the same numbers of cells in y and z direction. Similarly S6 through S9 and S10 through S13 were designed to study the effects of refinement along the y and z directions by keeping the same number of cells in the remaining two directions. In order to make the simulations comparable, they all had the same input data. After preliminary analysis, it was observed that the grid refinement is extremely necessary in y and z direction but not so much in x direction. Further observations and detailed result comparisons for this study would be discussed in the results section of this paper.

2.2. Fracture transmissivity

Another issue that is usually encountered while creating a simulation model is to decide on the width and permeability of the fracture. The fluid flowrate in the fracture is governed by the fracture transmissivity, which is the product of the fracture width times the fracture permeability (hydraulic conductivity). It is proposed that, as long as the fracture transmissivity remains constant, the same results should be obtained from the simulations. Meaning a

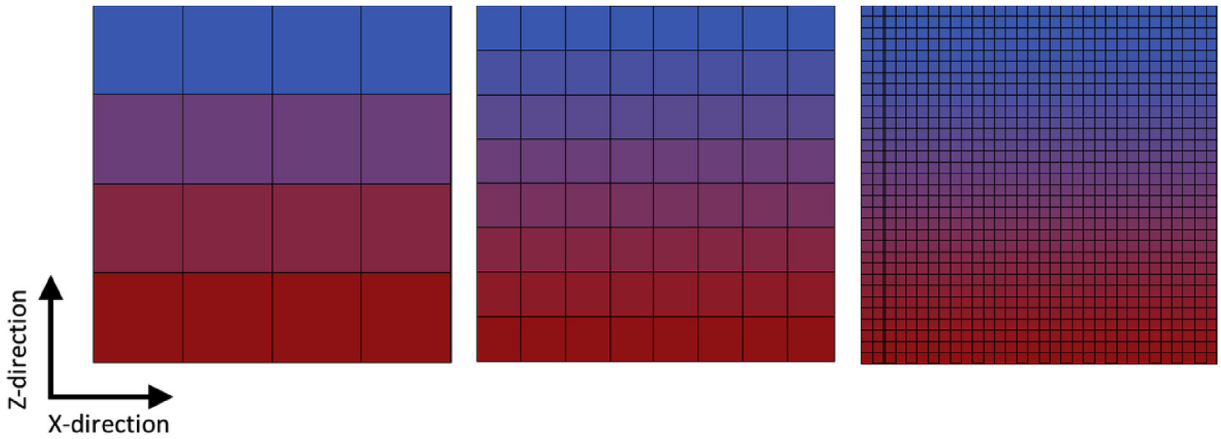

Fig. 3. Different grids from coarse to fine in x-z plane.

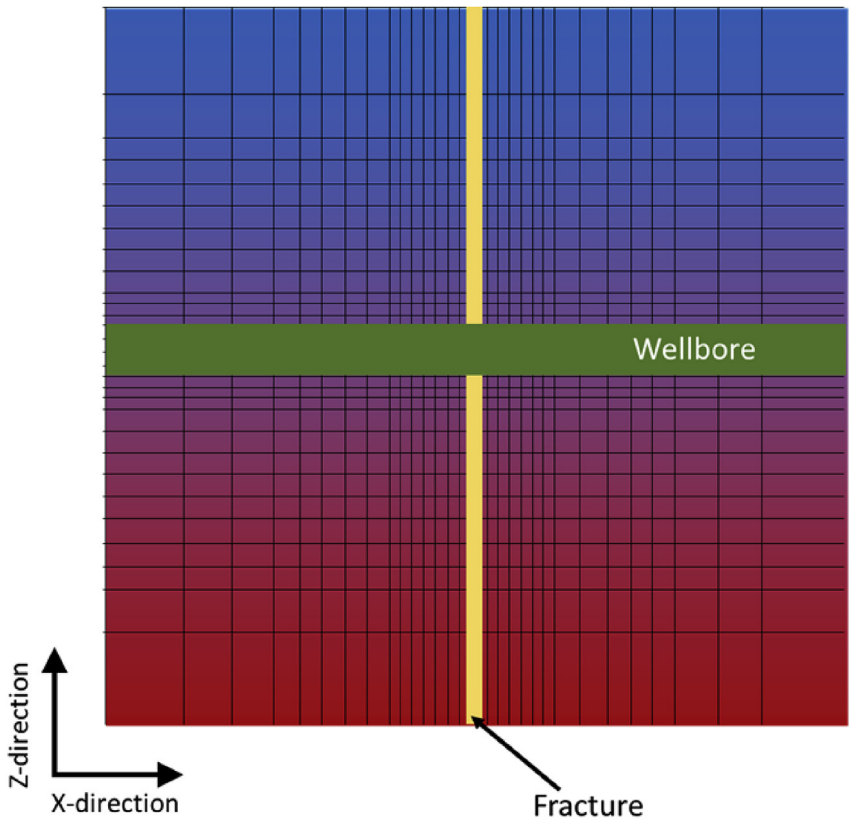

Fig. 4. Variation in grid size from near fracture to away from fracture.

0.001 m wide fracture with a permeability of 500000 mD (fracture transmissivity of 500mD.m) would yield similar results with fracture width of 0.1 m and fracture permeability of 5000 mD (fracture transmissivity of 500mD.m). To validate this, simulations were carried out for different combinations of fracture width and fracture permeability keeping the fracture transmissivity as constant. For the simulations, the fracture transmissivity of 500mD.m is used as shown in Table 2. The simulation were designed based on S3 from the previous study for grid refinement to.

After analyzing the results, it was proved that as long as the transmissivity of the fracture is kept constant, there is no effect on the temperature decline curve. The results are further discussed in detail in the result section.

3. Proposed model

To understand the working of EGS to produce hot fluid, we first need to understand the flow of heat inside the formation and the heat flow between the fracture and the formation.

3.1. Heat transfer in the system

According to studies performed by Cheng et al. [24] and Wu et al. [25], a heat transfer model for planar horizontal fractures (ideal geometry) can be created for a closed system. This model can be modified for a vertical fracture with a uniform gradient considering a pseudo 3D fracture model. It was assumed that the

Table 1
Grid Sensitivity in x, y and z directions.

Refinement Sensitivity	Simulation Number	Number of Cells in x-direction	Number of Cells in y-direction	Number of Cells in z-direction
Sensitivity in X-direction	S1	36	77	367
	S2	42	77	367
	S3	**58**	**77**	**367**
	S4	90	77	367
	S5	118	77	367
Sensitivity in Y-direction	S6	58	7	367
	S7	58	19	367
	S8	58	33	367
	S3	**58**	**77**	**367**
	S9	58	111	367
Sensitivity in Z-direction	S10	58	77	94
	S11	58	77	140
	S12	58	77	184
	S13	58	77	250
	S3	**58**	**77**	**367**

Table 2
Fracture transmissivity.

Simulation Number	Fracture width (m)	Fracture Permeability (mD)	Fracture Transmissivity (mD-m)
1	0.005	100000	500
2	0.01	50000	500
3	0.015	33333.33	500
4	0.02	25000	500
5	0.025	20000	500

fracture walls have constant surface area with no fluid losses to the formation. All the thermal properties including thermal conductivity of rock/fluid and heat capacity were assumed to be constant. The heat transfer inside the fracture considering heat storage, convection and conduction is given as shown in Equation (1).

$$\frac{\partial T(x,z,t)}{\partial t} + \overline{v_z}\frac{\partial T(x,z,t)}{\partial z} = \frac{2K_r}{\rho_w c_w b}\left.\frac{\partial T(x,z,t)}{\partial x}\right|_{x=0} \quad (1)$$

In this equation, $'\rho_w'$ is density of water, $'\overline{v_z}'$ is the average velocity of fluid in the fracture, $'c_w'$ is the heat capacity of water, $'b'$ is the average width of the fracture, $'K_r'$ is the thermal conductivity of the rock and $T(x,z,t)$ represents the temperature of the fluid and the formation (as both media need to be continuous).

The heat conduction in the rock is governed as shown in Equation (2). Here $'\rho_r'$ is density of the formation, and $'c_r'$ is the heat capacity of the formation.

$$\frac{\partial^2 T(x,z,t)}{\partial x^2} + \frac{\partial^2 T(x,z,t)}{\partial z^2} = \frac{\rho_r c_r}{K_r}\frac{\partial T(x,z,t)}{\partial t} \quad (2)$$

These equations are solved using numerical methods to get the decline curve for the produced water temperature from the individual fractures. CMG STARS is capable of solving these equations and obtaining the decline curves for any given model.

The decline curves for the temperature of produced water from each individual fractures (for Case 6 in Table 4) are shown in Fig. 5.

Fracture 1 represents the top most fracture and fracture 11 represents the bottommost fracture in the system. It can be observed that the temperature decline curve for each fracture follows a similar trend (except for fracture 1 and 11). The shift in each curve is because of the different fracture locations which are in different temperature zone due to the presence of temperature gradient in the reservoir. The fracture 1 and 11 have infinite reservoir on one end and a fracture on the other (see Fig. 6). Hence their decline curve appears to be different from remaining fractures. However, when average temperature of the produced water is calculated, the temperatures from the first and last fracture

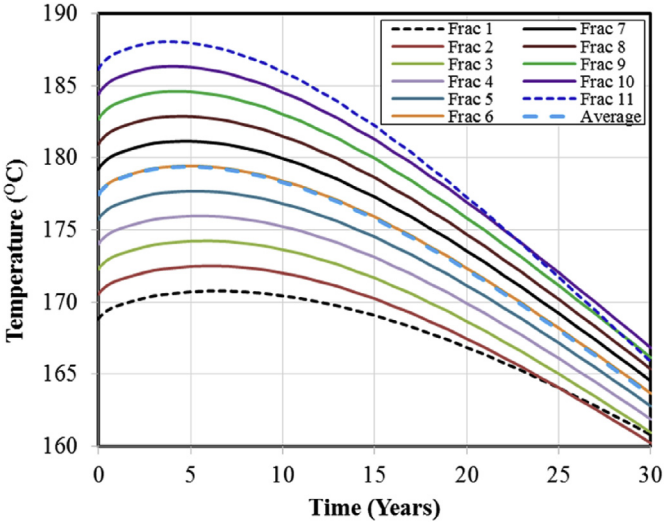

Fig. 5. Temperature decline curve for inidividual fractures in the reservoir.

balance each other. Also the average temperature curve follows the similar trend as the other curves. Hence, a simplified model of the entire reservoir can be created where we can get the decline curve for the system by just simulating some selective fractures from the system.

3.2. Downscaling the reservoir model

Following the lead from the above observations in Fig. 5, a downscaled reservoir model for EGS is proposed here.

To study the performance of an EGS in terms of temperature decline or energy extracted over time requires us to simulate the entire reservoir which consists of huge number of cells in all the directions. This would take a significant amount of time to build

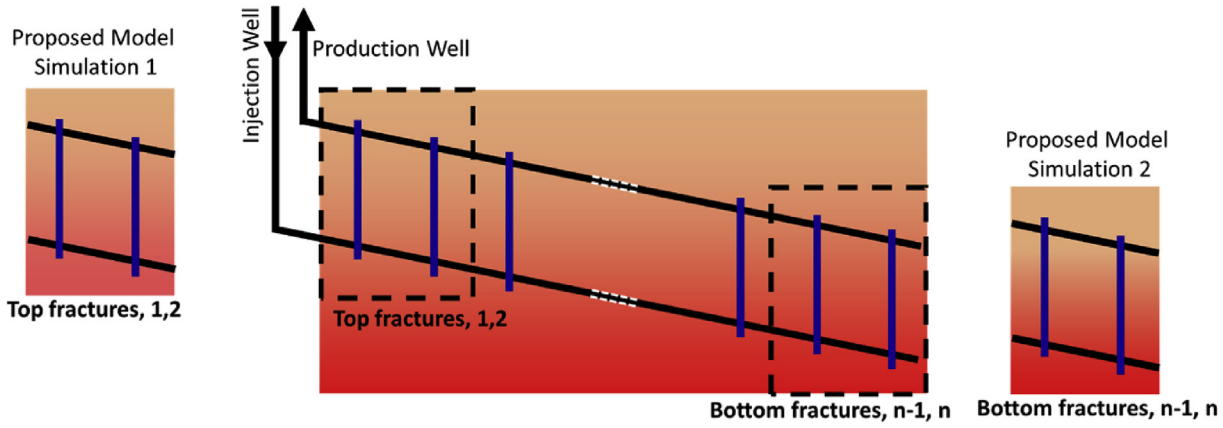

Fig. 6. Schematic diagram of the proposed model: top two fractures on the left (1st simulation of proposed model), entire reservoir in the middle, and bottom two fractures on the right (2nd simulation of proposed model).

and run, even with high computational capability. On the other hand, reduction in the number of cells would produce inaccurate results, as discussed in earlier sections. As multiple simulations are required to study the effects of different parameters, it would become quite time consuming to do the simulations this way.

A better approach to this problem is to downscale the simulation to simulate one or two small sections (depending on the inclination of wells) of the entire model, instead of simulating the entire reservoir. The downscaled model can be simulated using CMG STARS and the simulation results will be up-scaled to obtain the results for the entire reservoir. This would save time and would not require much computational capabilities.

A reservoir with dimension 500 m along the x-axis, 400 m along the y-axis and the height of the reservoir along the z-axis (depends on the inclination of the well and well spacing) is considered. Then two small sections of the reservoir can be simulated instead of simulating the entire reservoir. In the proposed model, two fracture zones, namely the top two fractures, or 1st and 2nd fracture, and bottom two fractures, or $(n\text{-}1)^{th}$ and nth fractures, are simulated separately as top two and bottom two fractures instead simulating of entire *n* fractures (Fig. 6). The reason for choosing two fractures instead of one was to capture the thermal interaction between the two consecutive fractures. The top and bottom two fractures were chosen to develop the model because these two zones have the largest temperature difference in the system. As the rate of heat extraction between the fluid and reservoir mainly depends on the temperature difference, both zones will have a different heat extraction profile and different decline curve. No-flow boundary conditions are applied in this study. The reservoir is isolated from the surroundings by not allowing heat as well as fluid to flow into simulated reservoir through its boundaries. This is generally a practical consideration when faults exist around the reservoir. The height of the reservoir was sufficient enough to make sure the temperature of the topmost and the bottommost layers did not change after 30 years.

The transmissivity of all the fractures is considered to be 500mD.m, and so as to keep the simulation grids in scale, the width of all the fractures was set to 0.01 m, which gives the permeability of 50000mD for all the fractures. Whereas any value can be chosen for the fracture width, 0.01 m was chosen in order to get a homogeneity in the grids for the simulation.

As we know the location of the fractures in the reservoir, the temperature zone (they lie in) can be calculated, and two individual simulations can be carried out. The other factors are kept the same as all the fractures are identical in nature. The flowrate in each fracture is calculated from the total well flowrate by assuming each fracture takes the same amount of fluid. Individual temperature decline curves are obtained from both the simulations and then analyzed together to produce the final results.

Using the proposed model, we obtain two different temperature decline curves, one for each simulation. Using these two temperature decline curves can be combined as per the Equation (3), to obtain the temperature decline curve for the entire reservoir, as shown in output section of Fig. 7.

$$\overline{\boldsymbol{T}}(\boldsymbol{t}) = \frac{1}{2}\left(\boldsymbol{T}_{1,2}(\boldsymbol{t}) + \boldsymbol{T}_{\boldsymbol{n}-1,\boldsymbol{n}}(\boldsymbol{t})\right) \tag{3}$$

In Equation (3), $\overline{\boldsymbol{T}}(\boldsymbol{t})$ is the temperature of the fluid calculated by the proposed model at a particular time *t*. $\boldsymbol{T}_{1,2}(\boldsymbol{t})$ and $\boldsymbol{T}_{\boldsymbol{n}-1,\boldsymbol{n}}(\boldsymbol{t})$ represent the temperature of the fluid obtained from the simulation for the top and bottom two fractures respectively, at the time *t*. This equation holds true for any reservoir which has a uniform temperature gradient (linearly varying temperature) along the depth of the reservoir. If the temperature gradient is linear, the rate of heat extraction also varies linearly with depth. So when both the end points (top and bottom) are considered, the difference in the rate of heat extraction due to difference in tempreature is taken into account, thus allowing us to predict the temperature decline curve for the entire reservoir by simulating two end points. According to the proposed model, the temperature decline curves obtained from two simulations are shown in Fig. 7 and the calculated decline curve is also plotted (Red Curve).

3.3. Verification of the proposed model

To establish the robustness of the proposed model, a wide range of important factors, namely, well inclination, well spacing and fracture spacing in geothermal system are selected. To evaluate the model performance, a range of these selected parameters was chosen from the lines of the data obtained from the FORGE site (shown in Table 3). The intermediate values closely represent the FORGE data and the maximum and minimum values were chosen accordingly.

To design an experiment with three parameters at three levels, the Box-Behnken design of experiment method [23] was chosen. Box-Behnken helps to reduce the total number of simulations required to be carried out and yet give accurate results. Using Box-Bhenken the total number of simulations was reduced from 27 to 13 (three parameters for three levels) simulations. These simulations are shown in Table 4.

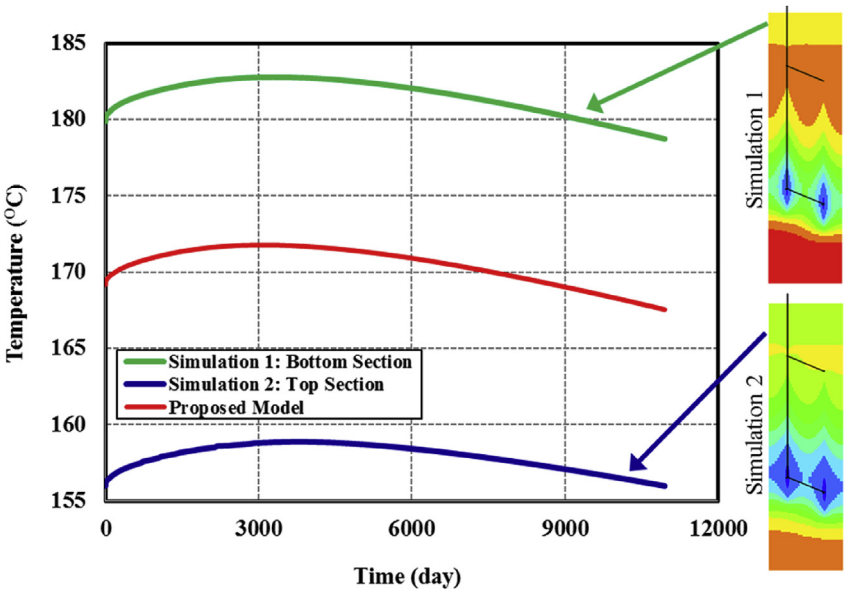

Fig. 7. Temperature decline curve for top zone (blue curve) and bottom zone (green curve) of the reservoir along with the calculated decline curve (red curve) for the entire model. (For interpretation of the references to colour in this figure legend, the reader is referred to the web version of this article.)

Table 3
Variable parameters.

Sr. no	Parameters	Maximum	Intermediate	Minimum
1	Well Inclination (1/degree)	90	60	45
2	Well Spacing (m)	300	200	100
3	Fracture Spacing (m)	100	50	25

Table 4
Box-Behnken design of experiments for three parameters.

Case	Well Inclination (degree)	Well Spacing (m)	Fracture Spacing (m)
1	45	100	50
2	45	200	25
3	45	200	100
4	45	300	50
5	60	100	25
6	60	200	50
7	60	100	100
8	60	300	25
9	60	300	100
10	90	100	50
11	90	200	100
12	90	200	25
13	90	300	50

While evaluating the robustness of the model over three important physical parameters for an EGS, the other parameters like the reservoir properties (thermal and geological), fluid properties, and fracture properties were kept as constant. Initial conditions and other properties are provided in Table 5.

Also to make sure that the experiment is on a comparative scale, the dimensions of the reservoir were kept constant. The dimensions of the entire model of the reservoir and its corresponding proposed model are noted in Table 6. The fracture height for the experiment was varied according to the well spacing to make sure that the injection and the production wells are connected.

In the case of horizontal wells, simulation of only one fracture zone at the toe of the well was sufficient to get the decline curve for the entire reservoir because all the fractures are identical and reside in the same temperature zone. For the inclined well, two zones are needed as all fractures reside in different temperature range.

Table 5
Physical properties of formation, fracture and fluid.

Parameter	Value
Density of the rock, kg/m^3	2700
Permeability of the formation, mD	0.01
Permeability of the fractured zone, mD	50000
Porosity of the formation, %	1
Porosity of the fractured zone, %	10
Initial water saturation, %	100
Thermal conductivity of formation, W/(m. °C)	3
Thermal conductivity of water, W/(m. °C)	0.591
Volumetric heat capacity of the formation, J/(m^3. °C)	2.133×10^6
Specific heat capacity of the fluid, J/(kg °C)	4818
Formation compressibility, 1/kPa	4.4×10^{-7}
Temperature gradient, °C/m	0.06
Reference depth, m	2520
Reference temperature (initial), °C	200
Reference pressure (initial), kPa	22000
Injection temperature, °C	80
Injection flowrate, m^3/day/fracture	100

The simulations were run for both the entire model and also for the proposed model to study the differences between the two. The time to run the entire model and time for the proposed model are recorded for comparison. Mean absolute percentage error (MAPE) and coefficient of determination (R^2) are calculated for error analysis.

4. Results and discussion

After running all the simulations, the results for grid sensitivity, fracture transmissivity and proposed model are discussed one by one in this section. The results are compared qualitatively (visual comparison) and quantitatively (calculating relative error) to evaluate the performance of the proposed model.

4.1. Grid sensitivity

In the grid sensitivity study, after running all simulations, the

Table 6
Comparison of dimensions of entire reservoir model and proposed model.

Dimensions	Entire Reservoir	Proposed Model
Reservoir length (X-direction), m	500	2 × Fracture spacing
Reservoir width (Y-direction), m	400	400
Reservoir height (Z-direction), m	510	510
Fracture width, m	0.01	0.01
Fracture half length, m		150
Fracture height, m	200-600 (Depends on well inclination and well spacing)	200-600 (Depends on well inclination and well spacing)

improvements in results due to finer grids is measured by the error calculations in terms of mean absolute percentage error (MAPE, See Appendix A) with respect to base case (Simulation S3) as shown in Table 7. The average error over 30 years of simulation was significantly affected in y and z direction but was negligible in x direction.

The Fig. 8 (a) shows the temperature decline curve for the produced water over 30 years, for five simulations with different grids along the x-axis. It was observed that all the temperature decline curves overlapped each other. Fig. 8 (b) shows the relative error for the decline curve with respect to simulation S3 (base case). The measured error for all the curves is negligible (maximum is 0.0003%) and acceptable while performing the simulations. It can be also observed that as the number of cells increases, the error reduced to zero.

Fig. 9 represents the temperature profile (after 20 years) for the cross section of the simulated zones with the different number of cells along the x-axis (x-z plane). It shows two fractures (grey lines) and the well bore connecting the fractures (pink lines), and the vertical black line representing the injection and production wells. Though the coarseness is observed visually with fewer cells, there is no major effect on the temperature decline curve, as long as some portion near the fracture is composed of refined grids (up to a few meters on both sides of the fracture to incorporate the near-fracture zone). This gives us the liberty of choosing fewer cells along x-axis, reducing the overall cells, and thus, the simulation time.

Fig. 10 (a) shows the temperature decline curve for the produced water over 30 years, for five simulations with different grids along the y-axis. As the number of cells increases along the y-axis, the temperature decline curve starts moving downward until no further changes are observed. This shows that the grids along the y-axis need proper refinement so as to get the accurate decline curve. Fig. 10 (b) shows the relative error for the decline curve with respect to simulation S3 (base case). The measured error for the curves is observed to be decreasing as we increase the number of cells along the y-direction. This shows that the temperature decline curve is quite sensitive to the number of cells along the y-axis.

Fig. 11 represents the cross section of the simulated zones with different numbers of cells along the y-axis (y-z plane). It illustrates the temperature profile (after 20 years) along the cross section of a fracture (black rectangular box). The white dot indicates the production well and the grey dot indicates the injection well. As the number of cells along the y-axis are increased, we can see a refinement in the temperature profile. As the fluid is flowing inside the fracture along the y-direction, it is important to ensure that the grids are properly refined. However, too many fine grids would give rise to a huge number of cells, thus increasing the simulation time. Therefore, it is important to choose optimum grid size.

The Fig. 12 (a) shows the temperature decline curve for the produced water over 30 years, for five simulations with different grids along the z-axis. As the number of cells increases along the z-axis, the temperature decline curve starts rising until no further changes are observed. This shows that the grids along the z-axis require proper refinement so as to attain the accurate decline curve. Fig. 12 (b) shows the relative error for the decline curve with respect to simulation 3 (base case). The measured error for the curves is observed to be decreasing as we increase the number of cells along the y-direction. This shows that the temperature decline curve is sensitive to the number of cells along the z-axis.

Fig. 13 represents the temperature profile (after 20 years) for the cross section of the simulated zones with the different number of cells along the z-axis (x-z plane). It shows two fractures (grey lines) and the well bore connecting the fractures (pink lines), and the vertical black line representing the injection and production wells. As the number of cells along the z-axis are increased, we can see a refinement in the temperature profile. As the fluid is dominantly flowing inside the fracture along the z-direction, it is important to make sure that the grids are properly refined. In Fig. 13, the temperature profile for 94 cells along z-axis shows that the area near the production well is still at $182^{\circ}C$—$188^{\circ}C$ but with 367 cells along z-axis, the area near production well is at $177^{\circ}C$—$182^{\circ}C$. This shows that if there is not proper refinement along the z-axis, the temperature distribution for the reservoir would be compromised, which then would yield an inaccurate temperature decline curve over time. But again, too many fine grids would give rise to a huge number of cells, thus increasing the simulation time. Hence it is important to choose optimum grid size along the z-axis.

Table 7
MAPE in temperature of produced water with respect to the base case.

	Simulation Number	MAPE (%) with respect to base Case 3
X -grid	S1	0.002
	S2	0.002
	S4	0.002
	S5	0.003
Y-grid	S6	0.048
	S7	0.008
	S8	0.005
	S9	0.001
Z-grid	S10	0.893
	S11	0.870
	S12	0.034
	S13	0.018

4.2. Fracture transmissivity

After running five different simulations with different combination of fracture width and fracture permeability (keeping transmissivity constant), it was observed that there is no major difference in the results. Fig. 14 shows the temperature decline curve for these five simulations.

It was observed that all of the 5 curves overlapped each other with negligible errors. This proves that the change in fracture width or fracture permeability, keeping the fracture transmissivity as a constant, does not affect the temperature decline curve over time. Moreover it does not affect the simulation time either. But when the fracture size is chosen to be large enough it does affect the results because the whole fracture acts like a coarse grid and might create discrepancies. Though this problem can be tackled by

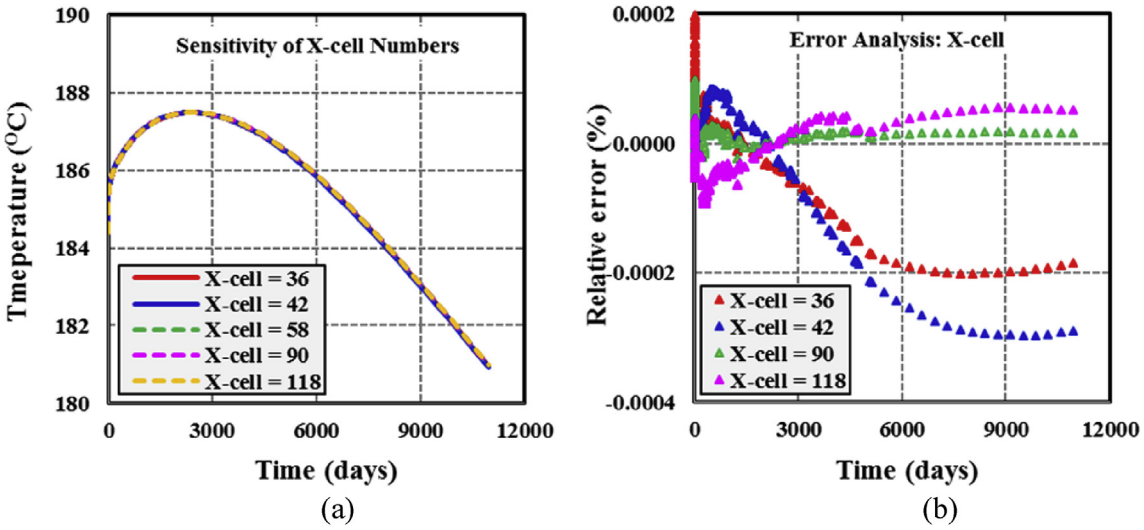

Fig. 8. Effect of different grids in x-direction on (a) temperature of produced water with time, and (b) error in comparison to the base case.

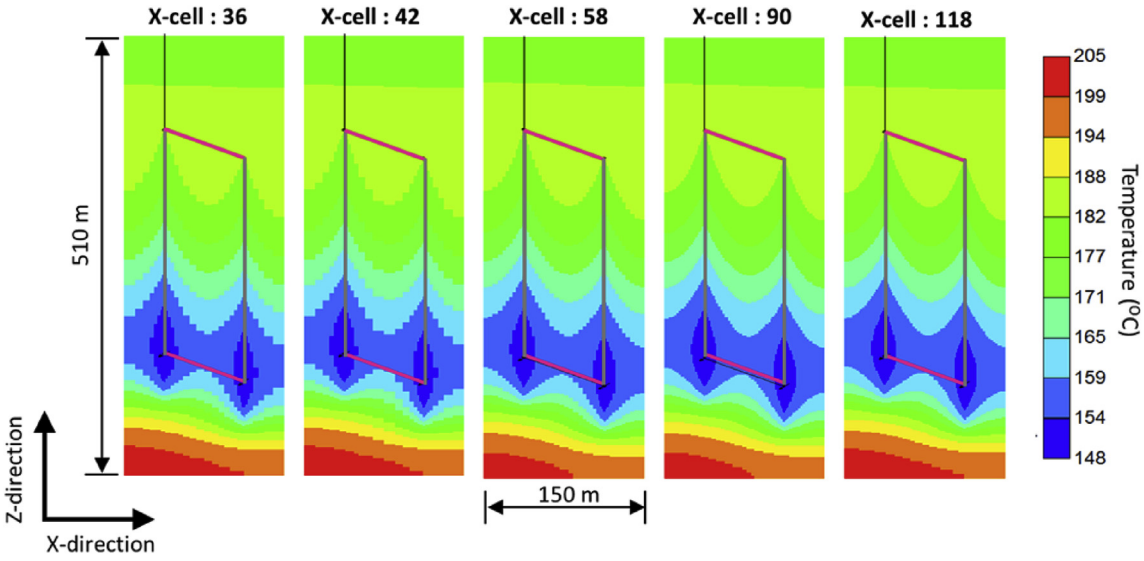

Fig. 9. Spatial distributions of temperature on x-z plane with different numbers of grid in x-direction (not to scale).

introducing refined grids within the fractures, this would increase the simulation time. So it is preferable to avoid wider fractures and choose a smaller fracture width with increased permeability, thus generating the same results as the previous case, provided the fracture transmissivity is kept constant. This proves that as long as the transmissivity of the fracture remains constant, we can pick any random values for the width of the fracture (changing the permeability of the fracture accordingly).

4.3. Proposed model

Before discussing the results quantitatively, qualitative comparisons of proposed model and the entire model are shown in Fig. 15. It shows the temperature profile (x-z plane) for the entire model and the proposed model.

Spatial distributions of temperature on x-z plane from proposed model and entire reservoir after 10 years is shown in Fig. 15. It was observed that the simulation using the proposed model (simulation of bottom two and top two fractures) showed similar temperature profile for the fractures when compared to the simulation results for the entire reservoir. This shows that the proposed model is an accurate representation of the entire model for the simulated factures. And hence, the results from the proposed model can be interpolated to get the temperature decline curve for the entire reservoir.

Table 8 illustrates the quantitative comparisons for the proposed model and the entire reservoir model. It shows the total number of cells simulated in each case, the time taken to run the simulations, and the error calculated for temperature decline curve for the proposed model with respect to the entire model.

It was observed that as the total numbers of cells in the proposed model are fewer than the cells required in the entire reservoir model, it requires much less time to run the simulations. Fewer cells also mean that the computational ability required to run the simulation would also be less. Additionally, the MAPE values for the proposed model are quite low and hence in the acceptable range and the R^2 values are close to 1. This tells us that the proposed model is an accurate representation of the entire model which

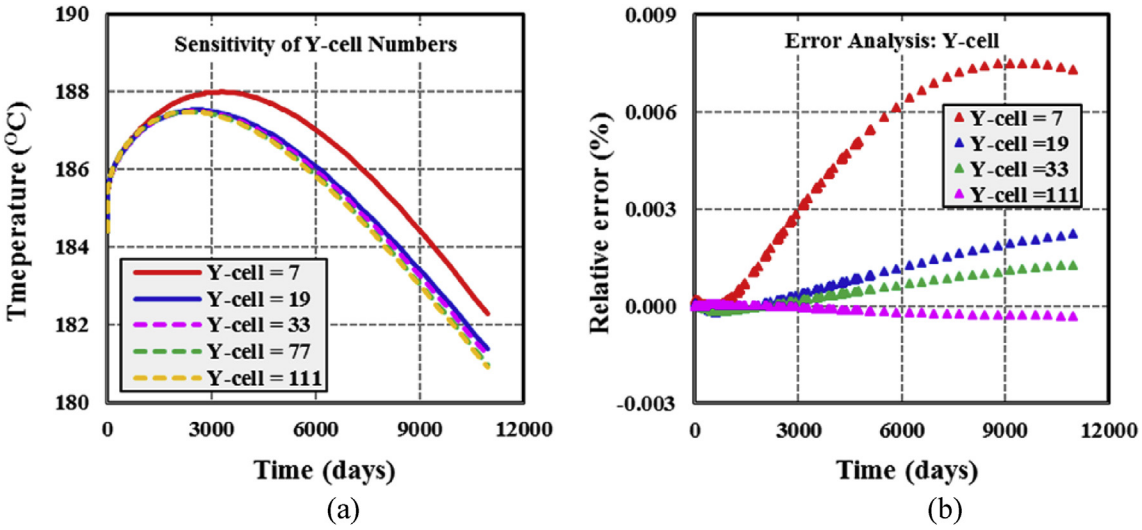

Fig. 10. Effect of different grids in y-direction on (a) temperature of produced water with time, and (b) error in comparison to the base case.

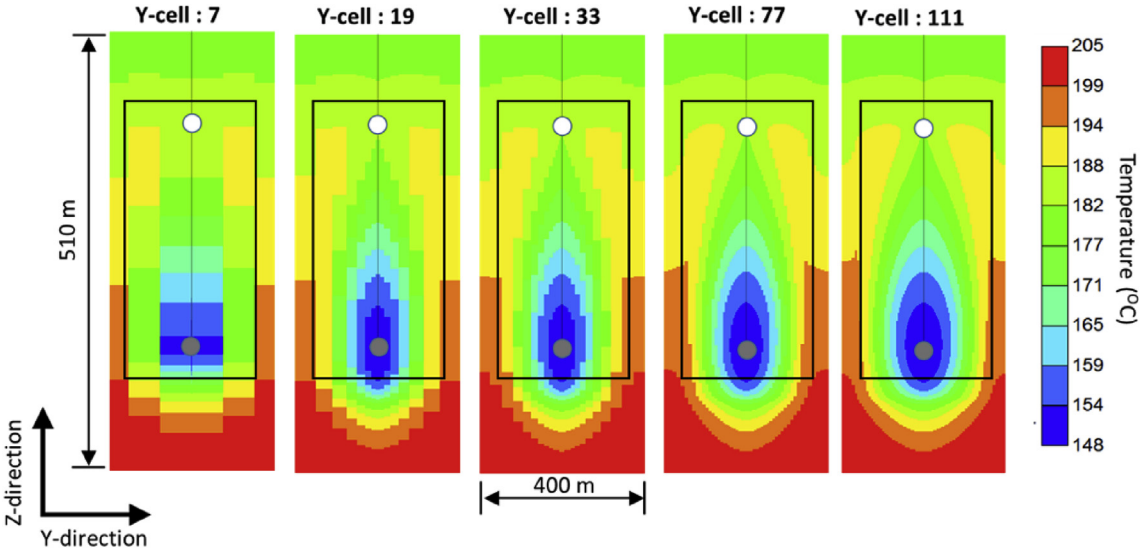

Fig. 11. Spatial distributions of temperature on y-z plane with different numbers of grid in y-direction (not to scale).

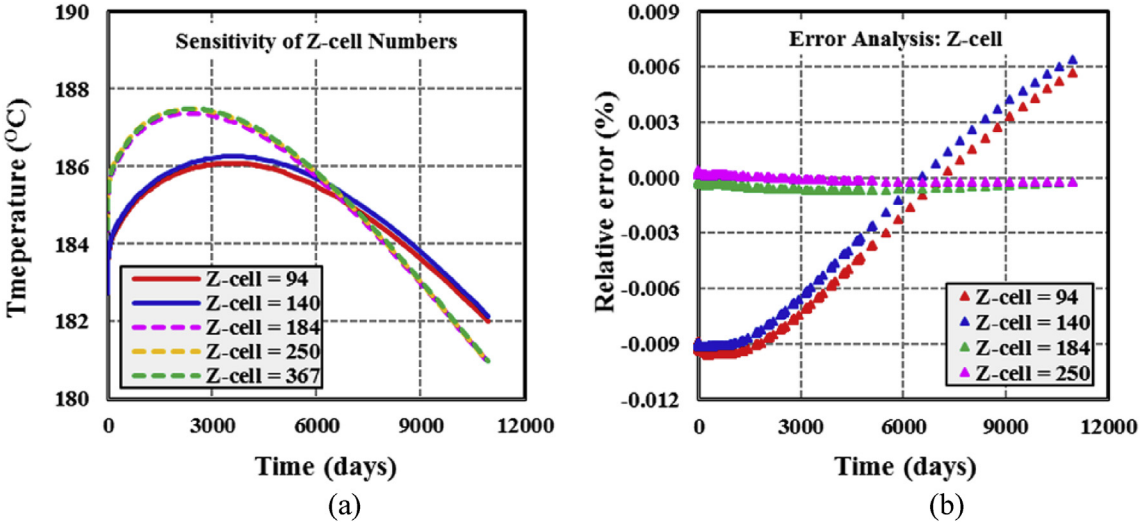

Fig. 12. Effect of different grids in z-direction on (a) temperature of produced water with time, and (b) error in comparison to the base case.

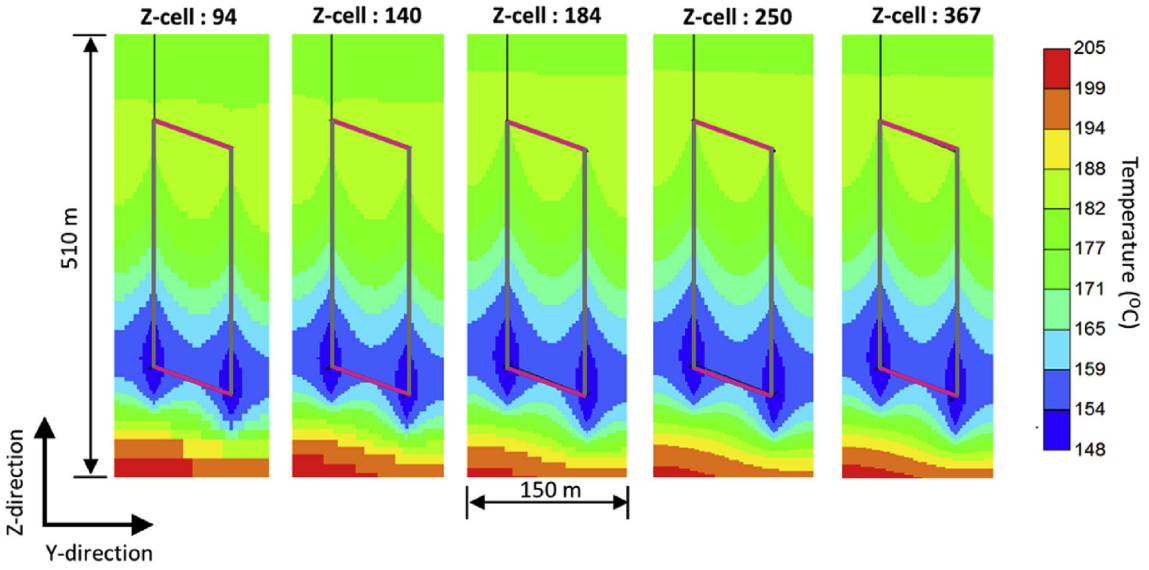

Fig. 13. Spatial distributions of temperature on x-z plane with different numbers of grid in z-direction (not to scale).

requires less time to simulate, low computational capabilities, and low memory requirements. In the case of horizontal wells, where only one zone of two fractures needs to be simulated, the simulation time is even less.

To maintain the baseline, the flowrate of 100 m^3/day/fracture was maintained in all cases for the proposed model and the entire reservoir. Fig. 16, shows the temperature decline curve for the production of water from the EGS, over 30 years.

The solid line represents the temperature decline curve for the entire reservoir, whereas the dotted line represents calculated temperature decline curve from the proposed model. It was observed that the proposed model for the EGS system, where only one or two fracture zones (consisting of two fractures) were simulated, gave accurate results throughout the life of the well with a maximum deviation of two to three degrees Celsius from the actual simulation for the temperature decline curve. In almost all the cases, the temperature decline curves for the proposed models exactly overlapped on the temperature decline curves for the entire reservoir model. The error analysis (Table 8) showed that the relative errors are near to zero except for few cases where the relative error is less than 3%. The R^2 values were observed to be close to one, and the MAPE values were less than 3%. As shown in the Table 8, the proposed model was able to save a very significant amount of time by reducing the simulation time by 1.5–14.5 times for the given reservoir size. As our main purpose for running the thermal simulations for an EGS is to get an estimated temperature decline curve by studying the effect of various parameters, the proposed model serves an excellent tool to do so in an efficient manner.

Also, a significant reduction in time was observed at a cost of insignificant error. As the chosen reservoir size was just 500 m long (along x-axis), this model would be even more time efficient for evaluating larger reservoirs. This shows that the proposed model for the entire reservoir gives promising results, and is flexible enough to be applied to any doublet model at any inclination, fracture spacing, and well spacing, with negligible errors. It efficiently and effectively represent the entire reservoir as implied by the values of R^2 and Mean Absolute Percentage Error (MAPE) and Relative Error (RE), implying that the proposed model can be used to obtain the temperature decline curve without actually needing to simulate the entire reservoir.

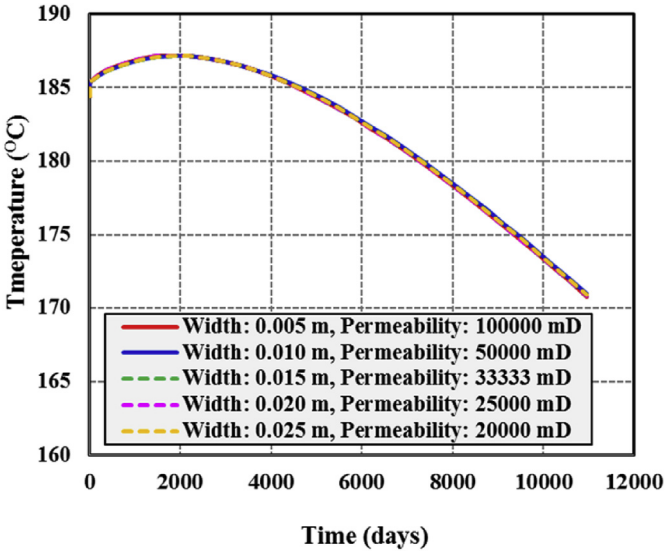

Fig. 14. Temperature of produced water for different combinations of fracture width and fracture permeability with same transmissivity.

5. Conclusion

This study focuses on the need for better, time efficient simulation of a doublet model for an EGS. Coarse grids render inaccurate results in less time, while finer grids give accurate results with more time. Choosing the optimum grid size with fine refinements near dynamic areas for the simulation is really important to obtain proper results that are more accurate and also time efficient. The direction along the well perpendicular to the fractures is least sensitive to the size of grids, but the plane of fracture is very sensitive because the fluid flow within the fractures is dominantly in y and z directions.

While simulating planar vertical fractures for a reservoir, the fracture width and permeability of the fracture together decides the flow through the fracture, and their product together is called the fracture transmissivity. When highly conductive fractures are required, it is advised to keep fracture width low (1 mm–10 mm) so that while modeling the system the refinements near the fractures

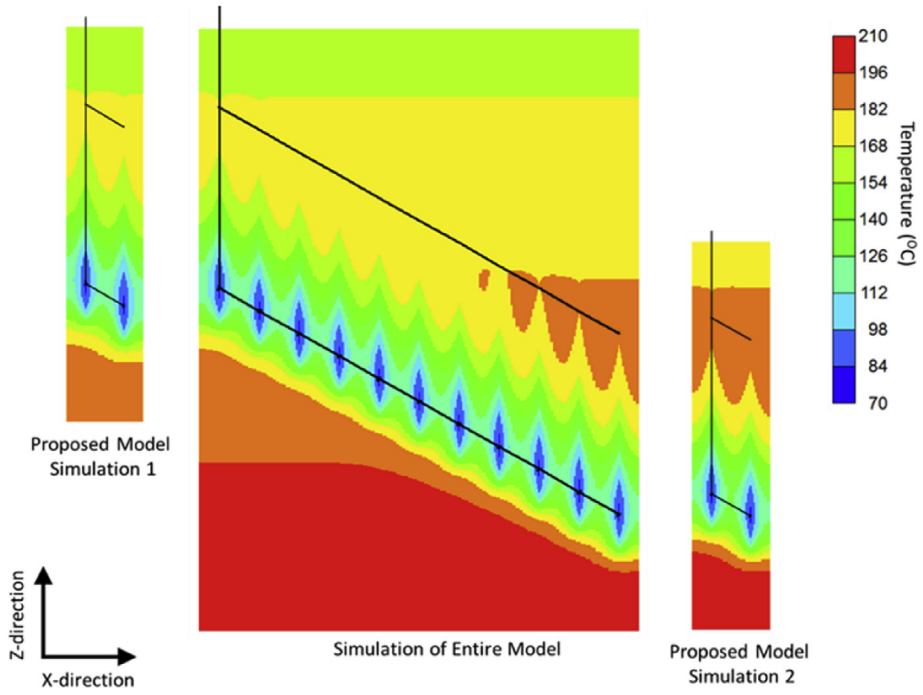

Fig. 15. Comparison of spatial distributions of temperature among simulation of top two fractures in the left (part of proposed model), simulation of entire field, and simulation of bottom two fractures in the right (part of proposed model), after time 3652 days in x-z plane.

Table 8
Comparison of entire reservoir model and proposed simplified model.

Simulation Number	Total Cells		Simulation Run Time (hrs.)			Error Analysis in Temperature	
	Entire Reservoir	Proposed Model	Entire Reservoir	Proposed Model	Improvement Factor	R^2	MAPE (%)
1	10927224	969892	12.0	3	4.00	1.00	0.51
2	19377512	772079	61.2	4.2	14.57	0.97	0.70
3	9281580	1794870	12.1	7.1	1.70	0.96	0.67
4	15491476	1955261	20.3	6.4	3.17	1.00	0.62
5	11235455	444444	18.9	2.3	8.22	1.00	0.35
6	11286968	1289750	13.5	4.5	3.00	1.00	0.21
7	5093550	964810	6.8	2.9	2.34	0.99	2.51
8	17568166	917378	34.9	6.1	5.72	0.99	0.21
9	8117340	2490180	11.0	7.5	1.47	1.00	0.22
10	2967888	680988	3.7	1.5	2.47	1.00	0.16
11	3751440	1250480	5.0	2.3	2.17	1.00	0.00
12	6099247	595441	11.9	1.8	6.61	1.00	0.21
13	6340488	1454838	8.8	2.7	3.26	1.00	0.02

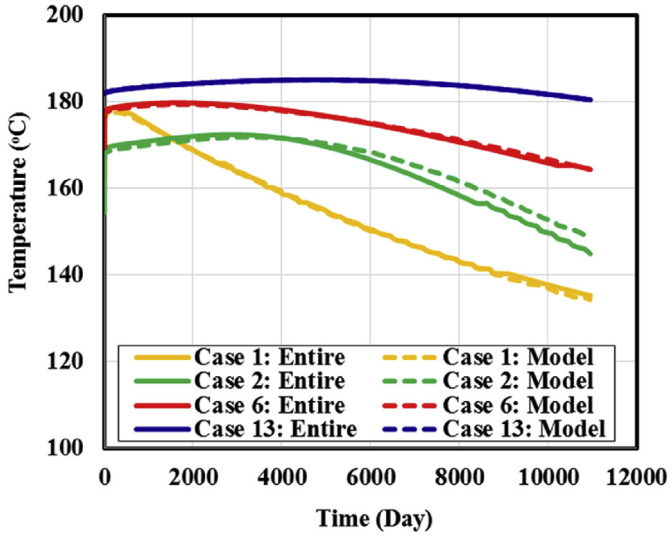

Fig. 16. Comparison of temperature decline curves for proposed model and entire reservoir simulation.

can be defined properly to avoid any discrepancies.

The proposed model for the doublet system of simulating the top and bottom zones of the entire reservoir can help predict the temperature decline curve for the whole reservoir without simulating it in full. The results obtained this way are highly accurate (0–3% error) and 1.5–14.5 times more time efficient. The model is robust and can be used for any well spacing, fracture spacing, and for the wells at any angular orientation.

EGS is a fairly new topic and is expected to be in demand soon with the need for efficient and sustainable power generation systems, as it has a reduced carbon footprint. This proposed model can be extremely useful when large numbers of simulations are to be carried out for a particular EGS, improving the study and optimization of simulations to render the most efficient system.

Acknowledgement

Funding for this project was provided by the U.S. Department of Energy, Office of Energy Efficiency & Renewable Energy under grant DE-EE0007080. We are grateful for their support.

Nomenclature

Symbol	Description	Units
$Y_{obs,i}$	Observed output in ith experiment	Unit of Output
$\overline{Y}_{obs}$	Mean of Observed Output	Unit of Output
$\overline{v_z}$	Average velocity of fluid in fracture	m/sec
K_r	Thermal conductivity of formation rock	J/m/s/°C
$\overline{T}$	Temperature of produced water from proposed model	°C
$Y_{model,i}$	Model Prediction of output for ith experiment	Unit of Output
c_r	Heat capacity of formation rock	J/kg/°C
c_w	Heat capacity of water	J/kg/°C
ρ_r	Density of formation rock	kg/m^3
ρ_w	Density of water	kg/m^3
EGS	Enhanced Geothermal System	–
FORGE	Frontier Observatory for Research in Geothermal Energy	–
HDR	Hot Dry Rock	–
MAPE	Mean absolute percentage error	–
R^2	Coefficient of determination	–
RE	Relative Error	–
T	Temperature of geothermal system	°C
$T_{1,2}$	Temperature of produced water obtained from simulation of top two fractures	°C
$T_{n-1,n}$	Temperature of produced water obtained from simulation of bottom two fractures	°C
b	Average width of the fracture	m

Appendix: A

Among many error analysis techniques to evaluate the accuracy of models, coefficient of determination (R^2), relative error (RE), and mean absolute percentage error (MAPE) are selected in this study. The coefficient of determination, R^2, indicates the overall accuracy of a model considering the two residual errors: error between model values and observed values and error between model values and average observed values as shown in Equation (A.1),

$$R^2 = 1 - \frac{\sum_{i=1}^{n}\left(Y_{obs,i} - Y_{model,i}\right)^2}{\sum_{i=1}^{n}\left(\overline{Y}_{obs} - Y_{model,i}\right)^2} \quad \text{(A.1)}$$

The values of R^2 varies from 0 to 1. The values closed to unity are indication of the better fit of the model curve with observed data.

Absolute values of errors sometimes do not provide sufficient information about how large the errors are. To avoid this pitfall, relative error is measured at a particular point of a curve as shown in Equation (A.2).

$$RE(\%) = \frac{y_{obj,i} - y_{model,i}}{y_{obj,i}} \times 100 \quad \text{(A.2)}$$

Relative errors show the error in each point of a curve with respect to that particular point. To calculate an overall error of the model, a single valued error is needed which is mean absolute percentage error (MAPE) as shown in Equation (A.3).

$$MAPE = \frac{1}{N}\sum_{i=1}^{N}\left|\frac{y_{obj,i} - y_{model,i}}{y_{obj,i}}\right| \times 100 \quad \text{(A.3)}$$

Use of absolute values are of interest to avoid any nullification of positive and negative errors.

References

[1] D. Duchane, D. Brown, Hot Dry Rock (HDR) Geothermal Energy Research and Development at Fenton Hill, New Mexico Geothermal Heat Center Bulletin, 2002.

[2] M.C. Smith, R.L. Aamodt, R.M. Potter, D.W. Brown, Manmade Geothermal Reservoirs Technical Report No. LA-UR-75-953, CONF-750525–750526, Los Alamos Scientific Laboratory, New Mexico, USA, 1978.

[3] A.S. Batchelor, The creation of hot dry rock systems by combined explosive and hydraulic fracturing, in: Paper Presented at the International Conference on Geothermal Energy, 1982.

[4] J.W. Tester, D.W. Brown, R.M. Potter, Hot Dry Rock Geothermal Energy – a New Energy Agenda for the 21st Century, LA-11514-MS New Mexico, USA Los Alamos National Laboratory, 1989.

[5] A. Bataillé, P. Genthon, M. Rabinowicz, B. Fritz, Modeling the coupling between free and forced convection in a vertical permeable slot: implications for the heat production of an Enhanced Geothermal System, Geothermics 35 (2006) 654–682.

[6] An Evaluation of Enhanced Geothermal Systems Technology:Geothermal Technologies Program, Department of Energy, USA, 2008.

[7] Y. Xia, M. Plummer, E. Mattson, R. Podgorney, A. Ghassemi, Design, modeling, and evaluation of a doublet heat extraction model in enhanced geothermal systems, Renew. Energy 105 (2017) 232–247.

[8] M.D. Aliyu, H.-P. Chen, Optimum control parameters and long-term productivity of geothermal reservoirs using coupled thermo-hydraulic process modelling, Renew. Energy 112 (2017) 151–165.

[9] Y.C. Zeng, Z. Su, N.Y. Wu, Numerical simulation of heat production potential from hot dry rock by water circulating through two horizontal wells at desert peak geothermal field, Energy 56 (2013) 92–107.

[10] W. Huang, W. Cao, F. Jiang, Heat extraction performance of EGS with heterogeneous reservoir: a numerical evaluation, Int. J. Heat Mass Tran. 108 (2017) 645–657.

[11] K. Zhang, B.-H. Lee, L. Ling, T.-R. Guo, C.-H. Liu, S. Ouyang, Modeling studies for production potential of Chingshui geothermal reservoir, Renew. Energy 94 (2016) 568–578.

[12] B. Wu, X. Zhang, R.G. Jeffrey, A.P. Bunger, S. Jia, A simplified model for heat extraction by circulating fluid through a closed-loop multiple-fracture enhanced geothermal system, Appl. Energy 183 (2016) 664–1681.

[13] X. Song, Y. Shi, G. Li, Z. Shen, X. Hu, Z. Lyu, et al., Numerical analysis of the heat production performance of a closed loop geothermal system, Renew. Energy 120 (2018) 365–378.

[14] Computer Modelling Group, https://www.cmgl.ca/stars, Retrieved 2018.

[15] P. Asai, P. Panja, J. McLennan, J. Moore, Performance evaluation of enhanced geothermal system (EGS): surrogate models, sensitivity study and ranking key parameters, Renew. Energy 122 (2018) 184–195.

[16] P. Panja, T. Conner, M. Deo, Grid sensitivity studies in hydraulically fractured low permeability reservoirs, J. Petrol. Sci. Eng. 112 (2013) 78–87.

[17] P. Panja, T. Conner, M. Deo, Factors controlling production in hydraulically fractured low permeability oil reservoirs, Int. J. Oil Gas Coal Technol. 13 (1) (2016) 1–18.

[18] D. Sanchez-Rivera, K. Mohanty, M. Balhoff, Reservoir simulation and optimization of huff-and-puff operations in the bakken shale, Fuel 147 (2015) 82–94.

[19] D. Tran, L. Nghiem, L. Buchanan, An overview of iterative coupling between geomechanical deformation and reservoir flow, SPE-97879-MS, in: SPE International Thermal Operations and Heavy Oil Symposium, 1–3 November, Calgary, Alberta, Canada, 2005.

[20] A.C. Gringarten, P.A. Witherspoon, Y. Ohnishi, Theory of heat extraction from fractured hot dry rock, J. Geophys. Res. 80 (8) (1975).

[21] G.M. Shook, A. Suzuki, Use of tracers and temperature to estimate fracture surface area for EGS reservoirs, Geothermics 67 (2017) 40–47.
[22] S.K. Sanyal, S.J. Butler, An Analysis of power generation prospects from enhanced geothermal system, in: Proceedings World Geothermal Congress, 24–29 April. Antalya, Turkey, 2005.
[23] G.E.P. Box, D.W. Behnken, Some new three level designs for the study of quantitative variables, Technometrics 2 (1960) 455–475.
[24] A.H.D. Cheng, A. Ghassemi, E. Detournay, Integral equation solution of heat extraction from a fracture in hot dry rock, Int. J. Numer. Anal. Meth. GeoMech. 25 (13) (2001) 1327–1338.
[25] B. Wu, X. Zhang, R.G. Jeffrey, A.P. Bunger, S. Jia, A simplified model for heat extraction by circulating fluid through a closed-loop multiple-fracture enhanced geothermal system, Appl. Energy 183 (2016) 1664–1681.